Available online at www.sciencedirect.com
SCIENCE DIRECT®
Corrosion Science 46 (2004) 377–386
CORROSION SCIENCE
www.elsevier.com/locate/corsci

The early stage oxidation and evaporation of Mg–9%Al–1%Zn alloy

F. Czerwinski *

Development Engineering, Husky Injection Molding Systems Ltd., 560 Queen Street S., Bolton, Ont., Canada L7E 5S5

Received 26 November 2002; accepted 26 June 2003

Abstract

Thermogravimetric technique was used to determine the oxidation and evaporation behaviour of AZ91D magnesium alloys with 5 and 10 ppm of beryllium at temperatures between 200 and 500 °C. Depending on temperature and time, the alloy experienced protective or non-protective oxidation with linear or accelerated oxide growth kinetics. During reaction in an oxidizing atmosphere, the additions of beryllium delayed the transient from the protective to non-protective scale formation. In an inert atmosphere, increased beryllium contents reduced the magnesium evaporation rate.

Keywords: Magnesium alloys; AZ91D; C. Oxidation; MgO; Beryllium; Thixomading

1. Introduction

Magnesium and its alloys are known of their high affinity to oxygen. They are particularly prone to surface degradation during high temperature manufacturing stages such as melting, welding or heat treatment. As a result, various measures are undertaken to avoid a potential fire hazard, diminish material loses and ensure quality of manufactured parts. Liquid alloys are usually protected by SO_2 or SF_6 atmospheres covering bath surfaces which form a thin, coherent and stable film on the melt surface [1]. For protection of a solid alloy during heat treatment, the nitrogen atmosphere with reduced oxygen content below 5% was found to be effective

* Fax: +1-905-951-5365.
E-mail address: fczerwinski@husky.ca (F. Czerwinski).

0010-938X/$ - see front matter © 2003 Elsevier Ltd. All rights reserved.
doi:10.1016/S0010-938X(03)00151-3

Table 1
Chemical compositions of alloys examined by inductively coupled argon plasma mass spectrometer following ASTM E1097-97 (modified) and E1479-99 standards

	Mg	Mn	Si	Ni	Cu	Zn	Fe	Al	Be
Alloy A	Balance	0.34	<0.005	0.005	<0.001	0.59	0.002	8.94	0.0005
Alloy B	Balance	0.25	0.012	0.0006	0.003	0.69	0.002	9.24	0.0010

All values in wt.%.

[2]. The common feature of both the melting and heat treatment is a long-term exposure, typically of the order of several hours. The exposure time factor is essentially different for the novel technique of semisolid processing where the total residency time of Mg alloy within the closed barrel system, filled with argon, is reduced to several minutes [3].

It is of engineering interest, therefore, to examine the short-term reactivity of magnesium alloys in oxidizing and protective atmospheres.

2. Experimental details

Two alloy compositions, corresponding to the AZ91D grade with 5 and 10 ppm (±0.15 ppm) of beryllium and manufactured by Solikamsk Desulfurized Works, Solikamsk, were tested (Table 1). Thermogravimetric measurements were performed using coupons with a size of $8\times6\times1.5$ mm which were sectioned from the central part of the as-cast ingot and mechanically polished with a 2400 silicon carbide paper as the final stage. The Perkin Elmer TGA-7 apparatus was capable of accommodating a specimen with the maximum weight of 0.5 g and had a measurement accuracy of 1 μg. Weight change kinetics were recorded in laboratory air and flowing atmosphere of ultrahigh purity argon under isothermal conditions in the temperature range of 200–500 °C for time intervals up to 60 min. The specimens were inserted into a chamber at room temperature and heated at a rate of 100 °C/min. The observations of the oxide growth surfaces and cross-sections were conducted with scanning electron and optical microscopy.

3. Results and discussion

3.1. Substrate characterization

The structure of the as-cast ingot consisted of dendritic grains with their shape and size being dependent on the distance from the ingot surface. The average distance between secondary dendrite arms was in the range of 200–300 μm and the surface relief indicated the microsegregation inside the interdendritic cells. The microstructure consisted of the γ phase, being the intermetallic compound of $Mg_{17}Al_{12}$ and the α-Mg matrix, a solid solution of Al and Zn in Mg [3]. Under equilibrium conditions,

the solubility of Al in Mg is 11.5 at.% at 437 °C, but in as-cast alloys a solid solution below 437 °C is enriched only with 3–4 at.% of Al [4]. In addition to the major components, trace impurities of Mg_2Si particles with a Laves phase structure and a melting point as high as 1085 °C were detected. There were also Mn–Al compounds e.g. $MnAl_4$, $MnAl_6$, originating from a metallurgical rectification of the alloy.

3.2. Reaction in air

Typical oxidation kinetic curves in air, as-measured by thermogravimetric method, are shown in Fig. 1. At temperature of 197 °C the alloy exhibited protective behaviour and no weight gain was recorded in the accuracy range of the balance. The non-protective oxidation with linear kinetics was revealed at 410 °C. Further increase of the temperature to 437 °C caused accelerated reaction with oxygen after approximately 30 min. A common feature of all the reaction kinetics was the incubatory period when the alloy's oxidation rate was negligible.

The protective oxidation, revealed by thermogravimetric measurements, can be explained by formation of compact oxide films (Fig. 2(a)). It is accepted [5] that the growth of compact MgO films is controlled by solid-state diffusion through adherent oxide areas followed by the reaction with oxygen at the oxide/gas interface. A possible explanation of highly protective behaviour at this stage could be based on an assumption of epitaxial monocrystalline nature of thin oxide films and a lack of easy-paths for fast Mg transport which enforces the slow lattice diffusion. During growth, in addition to the uniform oxide thickening, the surface layer of the alloy experiences morphological changes, as well. The outward Mg ion diffusion, leading to the inward vacancy flux, creates voids at the metal/oxide interface which not only act as channels for the transport of Mg vapour, but also form the local stress risers contributing to film cracking. Another factor causing generation of tensile stresses

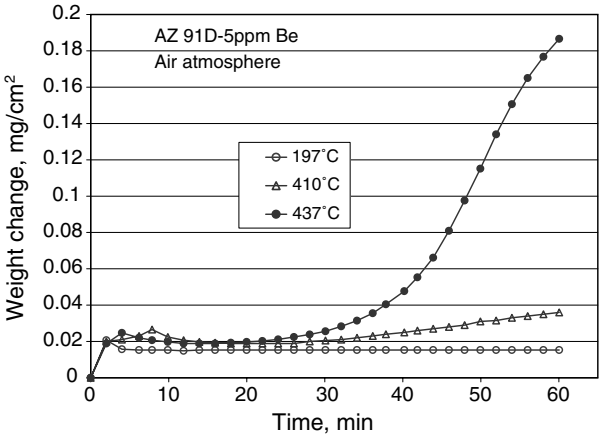

Fig. 1. The influence of temperature on oxidation kinetics of an AZ91D alloy with 5 ppm of beryllium in air atmosphere.

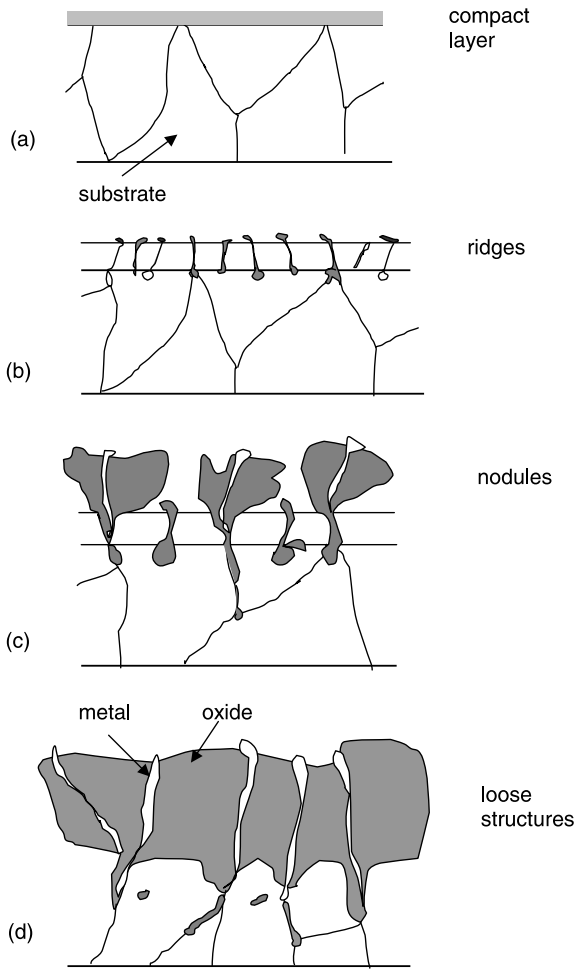

Fig. 2. Schematic representations showing development of MgO morphologies at various stages: (a) compact uniform layer; (b) transient to oxide ridges; (c) growth of oxide nodules; (d) loose scale structures.

and formation of fissures is the volume difference between the MgO film and metallic substrate. All those factors contribute to changes in oxidation kinetics.

The non-protective oxidation with linear reaction kinetics, e.g. at 410 °C, does not depend on the thickness of the scale and it is assumed that oxygen can easily penetrate to the metal surface (Fig. 2(b)). The morphology of oxide ridges, which replaces initial-stage structures and was described in details previously [6], is non-uniformly distributed over the alloy surface, and also does not show an obvious link with the substrate features. This type of structure indicates the formation of a fresh oxide at the oxide/metal interface, within the oxide and at the outer oxide surface. It is considered that the morphology is formed by inward oxygen transport through the cracks, followed by the reaction of oxygen with the metal at the crack walls and an

outward growth of ridges. A comparison of thermogravimetric kinetics and microstructure indicates that an onset of accelerated oxidation is associated with the growth of oxide nodules (Fig. 2(c)). The nodular growth is activated by phase inhomogeneity and in particular by the formation of liquid islands of the metal, increasing the Mg evaporation. Since the oxide grown during early stages is not uniform, a conversion of the weight gain to the oxide thickness can be used as estimation only. Further coalescence of nodules leads to continuous oxide scale with loose structure (Fig. 2(d)).

An example of oxide nodules is depicted in Fig. 3(a) and (b). Particularly at early growth stages (Fig. 3(a)), they contain a dark oxide with a bright contrast component which represents metal. The cross-sectional analysis shows the selective penetration of the oxide deep into the substrate because lower-melting point phases of the alloy experience preferential oxidation. The etching used to reveal structural components of the substrate in Fig. 3(c) made not visible the microchannels inside the oxide which connected the substrate with the nodule–gas interface. The microscopic

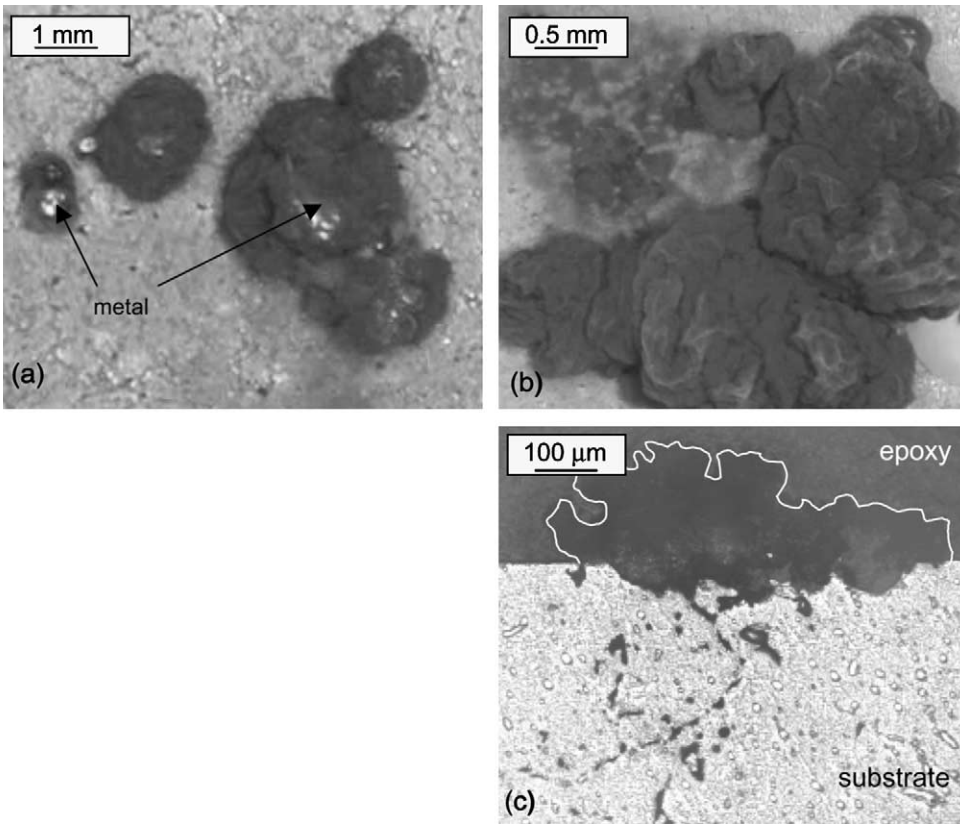

Fig. 3. Morphological characterization of oxide nodules: (a) top view, 472 °C—1 h; (b) top view, 497 °C—1 h; (c) cross-section, 527 °C—5 min after etching with nital.

observations indicate that nodules grow by the transfer of Mg vapour through voids and simultaneous reaction with oxygen, forming a product with cauliflower-like morphology. The mechanism is based on the saturation of scale pores by condensed metallic particles and their simultaneous reaction with oxygen and is also valid after the coalesced nodules form a continuous layer. It should be noticed that the selective oxidation of Mg results in the formation of the alloy depleted with respect to Mg (i.e. rich in Al) as the oxide moves inward to fill the space of the consumed metal. As proven by X-ray measurements [6], the oxidation of Mg to MgO is the predominant process and the direct reaction between Al and oxygen occurs only during combustion. During gradual oxidation, Al reacts to form $MgAl_2O_4$ spinel. The comparison of selected properties of metal matrix and oxides is depicted in Table 2. As seen in this table, there is a major difference between density of the metallic substrate of 1.8 g/cm^3 and oxide of 3.6 g/cm^3 which gives the Pilling–Bedworth ratio of 0.81. It explains that MgO will not form compact layer and systematic fissuring will occur.

It is well established that beryllium additions provide safety factor during melting and casting of aluminum and magnesium alloys. Beryllium is one of the few elements that is more reactive to oxygen than magnesium and it is known to getter iron and similar impurities from the melt, thus providing some degree of refinement in purity when needed [7]. The film forming characteristics of beryllium reduce moisture interaction and mold reactions. Exemplary oxidation curves for the AZ91D alloy with two Be contents are shown in Fig. 4. The initial stage up to roughly 10 min is quite similar for both alloys. During further exposure, additions of 10 ppm of Be significantly delayed the onset of accelerated oxidation stage and differences were substantial after roughly 10 min of reaction. More profound influence of beryllium is observed at higher temperatures as proved by observations of growth morphologies. After 1 h exposure at 500 °C, the alloy with 5 ppm of Be is entirely covered by the oxide scale (Fig. 5(a)) while the alloy containing 10 ppm of Be is still free of the oxide (Fig. 5(b)). After roughly 10 min at 547 °C, the alloy with 5 ppm of Be experiences ignition and combustion (Fig. 5(c)). An increase of Be content to 10 ppm delayed not only ignition but also oxidation (Fig. 5(d)).

Table 2
Selected properties of oxides formed on an Mg–9%Al–1%Zn alloy and the alloy's substrate

Material	Formula	Crystallographic structure	Density (g/cm^3)	Melting point (°C)	Thermal expansion coefficient (10^{-6}/°C)	Thermal conductivity (W/m °C)	Specific heat at 20 °C (J/kg °C)
Magnesia	MgO	Cubic	3.58	2800	8.0	40.6	837
Spinel	$MgAl_2O_4$	Cubic $a = 8.803$	3.60	2130	7.45		
Alumina	γAl_2O_3		3.60		8.0	21.0	880
Mg–9%Al–1%Zn substrate	αMg, $Mg_{17}Al_{12}$	Hexagonal close packed (αMg matrix)	1.81	499–603	27.2	56.2	800

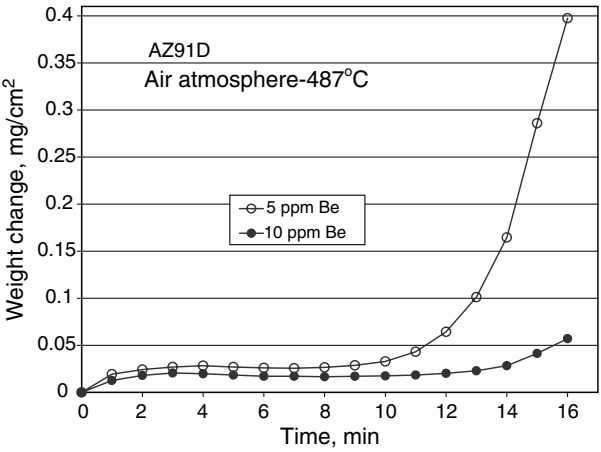

Fig. 4. The influence of beryllium content on oxidation kinetics of an AZ91D alloy in air.

At present, there is no experimentally proven mechanism which would explain the role of Be. A similar tendency was observed for other elements with high affinity to oxygen, as Ca, Sr or Zr. It is reported that elements with very high affinity to oxygen enhanced the formation of a thin and uniform oxide layer and prevented growth of thick nodular oxide features. It seems that the role of Be can be explained in terms of so called ''reactive element effect'' observed for NiO, chromia or alumina formers [8–10]. According to recent theory, the reactive element ions diffuse to native oxide grain boundaries and block the outward diffusion of metal cations. As a result, an inward diffusion of oxygen ions is the only possibility for the oxidation to proceed. For Ni substrate and Ce additions, a reduction in oxidation rate by roughly two orders of magnitude was achieved [8]. It is highly probable that similar mechanism can be active for the MgO growth. Since a certain concentration of reactive element ions at native oxide grain boundaries is required to impede diffusion this would explain a change in oxidation rate between 5 and 10 ppm of Be contents (Fig. 4).

3.3. Reaction in argon

The specific feature of Mg is the high vapour pressure and for vacuum environment its evaporation rate is described by the Arrhenius relation [5]:

$$K_{\text{evap}} = 0.6 \exp -\{25,000(\text{cal/mol})/RT\} \ \text{g/cm}^2\,\text{s} \tag{1}$$

According to a simple calculation, an evaporation of 1 μg/cm^2 of Mg translates to the removal of an approximately 55.3 Å thick metal layer. The higher the reaction temperature the more evaporation exceeds oxidation kinetically. For the Al–Mg alloy, at 500 °C the difference between evaporation and diffusion rate constants is over three orders of magnitude. The microstructure shows that above 437 °C, the Mg evaporation rate is so high that the vapour not only saturates all the pores within the

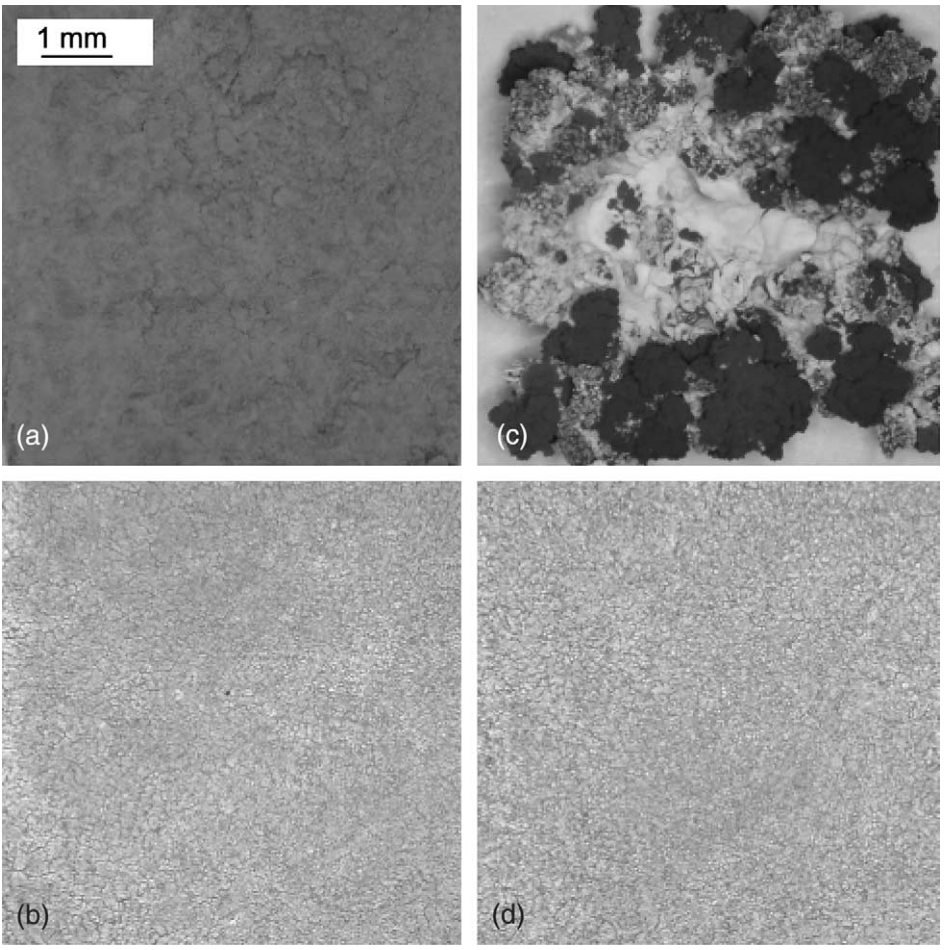

Fig. 5. Surface morphologies of an AZ91D alloys after high temperature exposures: (a) 5 ppm Be, 500 °C—1 h; (b) 10 ppm Be, 500 °C—1 h; (c) 5 ppm Be, 547 °C—10 min; (d) 10 ppm Be, 547 °C—10 min.

nodule but also reaches the nodule/oxygen interface where it forms a continuous film. It is suspected that for such a high evaporation rate, the reaction can even occur at a considerable distance from the surface and the resultant product would be released as incandescent MgO gas.

During experiments in an oxidizing environment, evaporation was superimposed on oxidation. To separate these two processes, alloys were exposed to high temperatures in an inert atmosphere of argon. The plot in Fig. 6 shows that during very initial stages, alloys with 5 and 10 ppm of Be experienced similar weigh gains which could be interpreted as an uptake of oxygen impurities. Then, beryllium suppressed the magnesium evaporation rate. Assuming that Mg evaporates from the metallic surface, according to Eq. (1) after 60 min at 487 °C, the sample weight reduction should be of the order of 100 μg/cm^2. The weight reduction, measured at this tem-

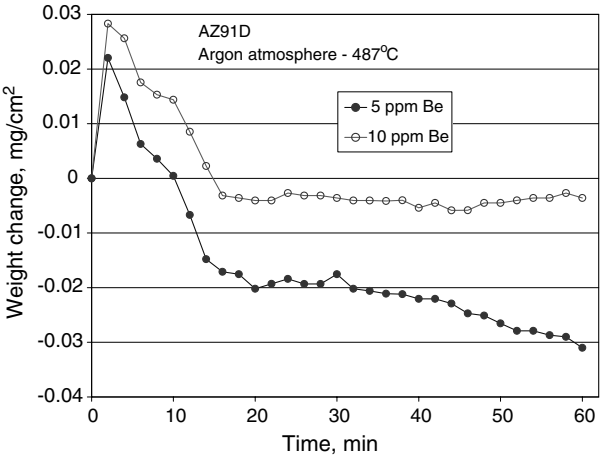

Fig. 6. The influence of beryllium content on weight change kinetics of an AZ91D alloy in argon.

perature by TGA is close to 50 μg/cm^2 (Fig. 6). A difference may be caused in part by experimental error and in part by a partial suppression of Mg evaporation by very thin oxide film, formed during first 10 min of exposure in argon. Magnesium may evaporate at an initial constant rate after the incubation period by two possible mechanisms: it may diffuse through the oxide film upon establishment of a concentration gradient or evaporate from the metal/vacuum interface if the compact oxide films breaks down to porous layer. The experiments show that the protective oxide formed tends to block the evaporation of Mg, while the loose high temperature oxide permits the evaporation to occur at a rate faster than that found at the beginning. The mechanism of evaporation suppression could be the same as explained in previous section for the reactive element effect on the oxidation inhibition.

4. Conclusions

The oxidation mechanism of Mg–9%Al–1%Zn alloys changes from protective to non-protective with linear or accelerated kinetics depending on the temperature and time of exposures. During reaction in an oxidizing environment, the beryllium addition delays the onset of non-protective oxidation. It does not affect, however, the oxidation kinetics during very initial stages. During reaction in an inert atmosphere of argon, beryllium suppresses the magnesium evaporation.

References

[1] S.P. Cashion, N.J. Ricketts, P.C. Hayes, J. Light Metals 2 (2002) 37.
[2] P.F. Stratton, E.K. Chang, in: H.I. Kaplan, J.N. Hryn, B.B. Clow (Eds.), Magnesium Technology 2000, TMS, Warrendale, PA, 2000, p. 71.

[3] F. Czerwinski, Adv. Mater. Process. 160 (11) (2002) 31.
[4] C.S. Roberts, Magnesium and Its Alloys, John Wiley & Sons, New York, 1960.
[5] W.W. Smeltzer, J. Electrochem. Soc. 105 (1958) 67.
[6] F. Czerwinski, Acta Mater. 50 (2002) 2639.
[7] ASM Metals Handbook, vol. 2, ASM International, Metals Park (OH), 1990, p. 426.
[8] F. Czerwinski, W.W. Smeltzer, J. Electrochem. Soc. 140 (1993) 2606.
[9] F. Czerwinski, J.A. Szpunar, Acta Mater. 46 (1998) 1403.
[10] F. Czerwinski, Acta Mater. 48 (2000) 721.